PLA/Carbon Nanotubes Multifilament Yarns for Relative Humidity Textile Sensor

Eric Devaux, Carole Aubry, Christine Campagne, Maryline Rochery

France Ensait, Gemtex Laboratory, Roubaix, FRANCE

Correspondence to :
Eric Devaux email : eric.devaux@ensait.fr

ABSTRACT

Polylactide (PLA) was mixed with 4 wt.% of carbon nanotubes (CNTs) to produce electrical conductive multifilament yarns by melt spinning process for humidity detection. Thanks to a variation of electrical conductivity, this flexible sensor could detect the moisture presence. The introduction of plasticizer was necessary to ensure higher fluidity and drawability of the blend during the spinning process. The plasticizer modifies the crystallinity and the mechanical properties of the yarns. The effectiveness of this sensor (PLA/4 wt.% CNTs fibres) sensitive to humidity, is optimal when the spinning conditions are adapted. In this way, the temperature and the rate of the drawing roll were reduced. The influence of these parameters on the crystallinity, the mechanical properties and the sensitivity of the yarns were studied. Once the appropriate spinning conditions found, one humidity sensitive yarn was processed and the repeatability and efficient reversibility of its sensitivity were highlighted.

INTRODUCTION

Polylactide (PLA) is a biodegradable polymer which is produced from renewable resources. A growing interest is also found for using this new polymer in many applications[1-2]. This polymer can be mixed with various fillers in order to enhance the inner properties such as thermal and fire properties[3-6]. Carbon nanotubes, discovered in 1991 by Iijima[7], are today considered as one of the most interesting filler in technology world due to the versatility of their potential applications. They can be used for instance to improve electrical[8-9], mechanical[10-11] properties or fire[12-13] resistance of polymer matrices. Dujardin *et al.*[14] and Dillon *et al.*[15] demonstrate the capillarity and wetting properties of multi-walled carbon nanotubes (MWNTs) and the gas storage in single-walled carbon nanotubes (SWNTs) respectively. Due to their very large adsorption capacity and the change of electrical resistance upon exposure to volatile molecules, carbon nanotubes (CNTs) can be used as chemical sensors[16]. Gases such as NO_2, CH_4, CO, CO_2, O_2, NH_3, H_2O and C_2H_5OH can act as a temporary p-dopant or n-dopant of the nanotubes corresponding to an increase or a decrease of the resistance of nanotube body and of the intertube tunnelling barrier[17-21]. For n-type MWNTs, the chemisorption of reducing gases (NH_3, H_2O) increases the electrical conductivity due to the increase in conduction band electrons. On the contrary for p-type MWNTs, the adsorbed reducing gas molecules donate electrons to the valence bond thereby increasing the electrical resistance[22]. To enhance the sensitivity of sensors based on nanotubes, Valentini *et al.*[23] introduce poly (*o*-anisidine) (POAS), an acid sensitive polymer, onto a CNTs device. In contrast to the CNTs device, the POAS modified CNTs sample exhibit higher electrical conductance modulation upon exposure to small concentrations of HCl in air. The use of polymer-nanotubes nanocomposites allows increasing the sensitivity but also the selectivity of the sensor. In fact, the particular sensitivity of polymers to gases molecules helps the sensor displaying high chemical selectivity[24]. The nature of the polymer depends directly on the selected gas to detect. In this way, poly (ethylene glycol) (PEG) showed high sensitivity to vapours of chloroform, ethanoic acid and water[24].

Poly (methyl methacrylate) (PMMA) enhanced sensitivity to water, dichloromethane, chloroform, acetone and hexane vapours[25-26]. In the case of PEG, the presence of these volatile molecules induces the swelling of the polymer, and the intertube distance between CNTs is enlarged leading to a large increase in electrical resistance of the blend. This effect is called the positive vapour coefficient (PVC)[27]. In contrast, in the case of PMMA, upon water exposure, the electrical resistivity decreases because of the increase of charge transfer. Because of the non-solvent effect of water for PMMA, no swelling of the polymer can be observed. The conductive path number increases in the presence of water. The electrical response of the CNTs-based polymer to a

number of gases seems to be related to the modification of the conductive network due to the swelling of the polymer and/or the charge transfer resulting from the interaction of adsorbed gas molecules with CNTs[28]. Kobashi *et al.* demonstrate recently the sensing properties of polylactide (PLA)/CNTs blends to several liquid solvent such as chloroform, tetrahydrofuran, toluene, n-hexane, dichloromethane, ethanol and water[29].

In a previous study, we produced monofilaments containing PLA and carbon nanotubes for humidity sensing. To obtain a very thin monofilament with sensitive properties, the content of CNTs has to be sufficient and close to the percolation threshold to obtain a variation of electrical conductivity as a function of humidity presence. The drawing effect during processing enhances the intertube distance and the appropriate drawing has to be determined to obtain a sufficient sensitive sensor. In this study, we had highlighted the content of CNTs (4%) in PLA to obtain an electrical conductive PLA monofilament. A percolation curve versus diameter for a PLA/4 wt.% CNTs monofilament was presented. A minimum diameter close to 80 µm was determined to keep a monofilament sufficiently conductive to maintain the sensitivity of humidity after drawing. PLA multifilament yarns can be produced by different ways such as melt spinning drawing process[30-33]. To produce electrical conductive PLA multifilament yarn, it is necessary to add at least 4 wt.% of CNTs. This high filler content can strongly increase the melt viscosity of PLA which is a limiting factor for melt spinning process. The introduction of plasticizer is consequently needed to spin this blend. The effects of plasticizer on the properties of PLA and PLA nanocomposites have also been largely investigated[34-38]. The addition of a suitable plasticizer such as poly (ethylene glycol) generally decreases the glass transition temperature of the polymer, the molecular mobility being improved. In this paper PLA was melt mixed with 4 wt.% of carbon nanotubes to elaborate a humidity sensitive multifilament yarn. The influence of plasticizer content in the PLA and PLA/4 wt.% CNTs composite was studied. Fluidity and thermal transitions were investigated on the nanocomposites after melt mixing whereas crystallinity, mechanical, electrical and humidity sensing properties were performed on the final multifilament yarns. Melt spinning conditions, as temperature and rate of the drawing roll, were also studied to optimize the thermal, mechanical and sensing properties of the yarn.

EXPERIMENTAL

Materials

Thin multi-wall carbon nanotubes (MWNTs) 90% purified were supplied by Nanocyl (Belgium) under the reference Nanocyl®-7000. Their main characteristics are diameter close to 10 nm and length between 0.1 and 10 µm with a surface area of 250 m^2/g. They are synthesized by catalytic chemical vapour decomposition (CCVD), which affords larger scale production and is a good compromise to get thus a lower cost for carbon nanotubes and a satisfactory degree of purity. Polymer used in this study is a semi-crystalline thermoplastic polylactide (PLA) reference NatureWorks®-6201 D from NatureWorks (Mn = 58300 g/mol; D-Isomer = 1.3%). Pellets were held at 80°C for 12 hours in order to remove any trace of water before extrusion and spinning. Liquid plasticizer Crosadd I-ASE (I-ASE), an alkylsulphonic phenyl ester, from Eurodye was used as PLA plasticizer. It was chosen for its high thermal stability.

Nanocomposite Preparation

In a first step, the carbon nanotubes were incorporated into the polylactide with a weight percentage of 15% and dispersed using a Thermo Haake co-rotating, intermeshing twin-screw extruder (L/D = 25). To facilitate dispersion of nanofillers in a polymer, the shear stress applied to the molten polymer has to be optimized, due to the residence time within the barrel. Thus, the screw rotational speed is fixed at 100 rpm. This extruder includes five heating zones in which the temperature is independently and gradually fixed from 140 to 190°C. In a second step, this masterbatch is diluted with PLA pellets to obtain concentration of 4 wt.% of carbon nanotubes in polylactide. During this second step, the plasticizer is incorporated through a second feeding zone in the middle of the extruder in proportion 5, 10 and 15 wt.% *Figure 1*. The material obtained is a monofilament (rod with 1.5 mm diameter) used directly for electrical and thermal measurements or pelletized and introduced in the spinning machine prior to obtain multifilament yarn.

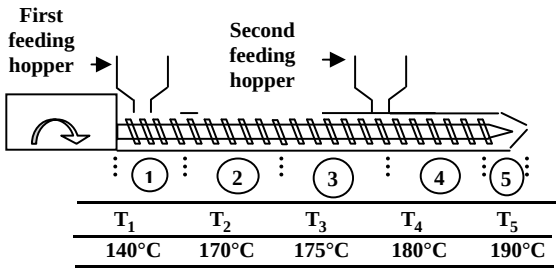

FIGURE 1. Extrusion process of PLA/CNTs/I-ASE blends.

A melt spinning machine called Spinboy I manufactured by Busschaert Engineering is used to spin-drawn multifilament yarns *Figure 2*.

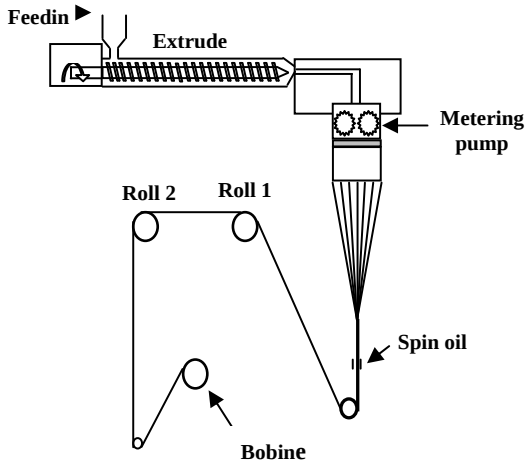

FIGURE 2. Melt spinning process of PLA and blends samples.

Pellets are first melted in a single screw extruder which includes five heating zones in which the temperature is independently and gradually fixed from 210°C to 215°C. Then, molten polymer passes through two dies consisting of 40 channels with a diameter of 400 µm each to produce a multifilament continuous yarn. The multifilament is covered with a spin finish which ensures the monofilaments cohesion along the process, rolled up on two heated rolls with varying speeds (S_1 and S_2) to ensure drawing. The theoretical drawing of multifilament is given by the draw ratio DR = S_2/S_1. During the melt spinning process, the polymer is stretched to favour the orientation of the constitutive macromolecules in the direction of the filament and to optimize the mechanical properties. PLA, PLA/I-ASE and PLA/4 wt.% CNTS/I-ASE multifilament yarns were produced. Various draw ratios (DR) were tested by changing both the feeding roll speed (S_1) and the drawing roll speed (S_2). The feeding roll temperature T_1 was fixed at 70°C and 2 different drawing roll temperatures (T_2) were applied. *Table I* shows the spinning conditions of the different yarns produced. As seen in previous studies[39], in order to obtain a conductive monofilament, a minimum diameter of 80 µm is required. To ensure the appropriate diameter for the monofilaments which compose the multifilament yarn, S_2 was decreased from 400 m/min to 150 m/min and 110 m/min. Each final monofilament had a diameter close to 90 µm and 115 µm respectively. The influence of this drawing roll speed on crystallinity and tensile properties PLA fibres were studied. For the low speed of the roll, the drawing roll temperature had to be reduced; T_2 was also decreased from 110°C to 90°C.

TABLE I. Component proportions and spinning conditions of the different fibres.

Sample	PLA (wt%)	I-ASE (wt%)	CNT (wt%)	S1 (m/ min)	S2 (m/ min)	T2 (°C)
P-1-90	100			125	150	90
P-2-90	100			150	200	90
P-3-90	100			200	300	90
P-4-90	100			200	400	90
P-1-110	100			125	150	110
P-2-110	100			150	200	110
P-3-110	100			200	300	110
P-4-110	100			200	400	110
PI5-4-110	95	5		200	400	110
PI10-4-110	90	10		200	400	110
PI10C4-0-90	86	10	4	100	110	90
PI10C4-1-90	86	10	4	125	150	90
PI15C4-0-90	81	15	4	100	110	90
PI15C4-1-90	81	15	4	125	150	90

Melt Flow Index Measurements

The Melt Flow Index (MFI) is a measurement of the molten thermoplastic polymer flowing. It is defined as the weight in grams of polymer flowing during 10 minutes through a capillary with specific diameter and length by a pressure applied via prescribed alternative gravimetric weights for alternative prescribed temperatures. The method is given in ASTM D1238 and ISO 1133 standards (similar). The MFI tests were carried out on a Melt Flow Rate (MFR) tester from Thermo Haake. The temperature applied during the test was 215°C for PLA filled with plasticizer and 250°C for PLA/4 wt.% CNTs filled with plasticizer. The applied load was fixed at 2.16 kg. Three MFI measurements per sample were made and the average was calculated and presented.

Thermal Characterizations

Differential scanning calorimetry (DSC) was carried out using a TA Instruments DSC 2920 under nitrogen atmosphere. Samples of 10 mg were heated from 20 to 200°C at 10°C/min and cooled to 20°C at the same rate. The glass transition temperature (T_g), cold crystallisation temperature (T_{cc}), melting temperature (T_m) and degree of crystallinity (X_c) were determined from the heating scan. For pellets samples, the first heating scan was meant to remove the effects of thermal history of the samples and the second heating scan was studied. However, for the multifilament yarns samples, the first heating scan was taken into account in order to show the spinning conditions influence on the PLA and blends crystallinity. T_m and T_{cc} were taken at the maximum peak value of the respective endotherms and exotherms, and the T_g at

the mid-point of heat capacity changes. Three measurements per blend were performed and the average value was presented.

Mechanical Tests Of Multifilament Yarns

The tensile properties measurements of PLA and blends fibres were carried out following the NF EN ISO 5079 standard on a tensile testing machine Zwick 1456, the cell force used being 10 N. All the tests were carried out at standard atmosphere, i.e. the temperature was 20 ± 2°C and the relative humidity was 65 ± 5 %. The length between the clamps was 20 mm. The results represent an average of 50 tests.

Electrical Conductivity Measurements

Electrical properties were measured using a Keithley 617 multimeter connected with alligator clips for rods and multifilament yarns. The length for measurement was fixed at 5 cm. 10 values per blend were carried out. The apparent applied voltage to the sample and current were measured.

The conductivity was calculated using the following equation:

$$U = RI,\ R = \frac{\rho\, x\, l}{S} \text{ and } C = \frac{1}{\rho} \quad (1)$$

where, U is the voltage (V), I is the current (A), R is the electrical resistance of the material (Ω), ρ is the resistivity (Ω.m), l is the length (m), S is the cross section of the material (m^2), and C is the electrical conductivity ($S.m^{-1}$).

Humidity Sensor Analyses

The dependence of the electrical properties of the multifilament yarns on climatic conditions was investigated with a climatic chamber Excal 2221-HA from Climats®. During the test, the temperature was kept constant at 25°C while the relative humidity (RH) was varied from 25% to 100%. The varying RH performed three consecutive complete cycles. The electrical resistance change of the samples was monitored using the same Keithley 617 multimeter as previously. The samples were placed at the centre of the chamber and connected to the instrument placed outside the chamber and interfaced with a computer to record electrical resistance (R) variations. Resistance values were collected every 3 RH% during 3 consecutive cycles. Based on these data the sensitivity of the different multifilament yarns was calculated as the Eq. (2):

$$S = (R_0 - R) / R_0 \quad (2)$$

where S is the sensitivity, R_0 the initial resistance at the beginning of the test (25°C, 25 RH%) and R the resistance at relative humidity RH%. In this paper, the third cycle of the sensing test is studied.

To study the sensitivity to high humidity atmosphere, the same sensitive fibres were tested in a 100 RH% area. Samples were first placed outside the climatic chamber, the room relative humidity was measured around 35 RH%. After electrical resistance measurement, the sample was placed immediately in the middle of the climatic chamber under 25°C and 100 RH% conditions. Resistance values were collected every 20 s. The sample was then removed and data always collected in order to evaluate the inertia of the phenomenon. Four consecutive cycles were tested to study the repeatability and reversibility of the signal.

RESULTS AND DISCUSSION

Melt Flowing Properties Of Blends

PLA and PLA/4 wt.% CNTs were tested with various contents of plasticizer. Because of the higher viscosity of PLA filled with 4% CNTs, the Melt Flow Index (MFI) of PLA/4% CNT were performed at higher temperature (250°C) than for the PLA without fillers (215°C). In both cases the introduction of plasticizer I-ASE increases the MFI value *Figure 3*, corresponding to a higher fluidity of the blend. The inclusion of the plasticizer in PLA polymer increases the mobility of macromolecular chains at the molten state. MFI gives indication about the melt flow behaviour of the polymer during the spinning process. The very high MFI value of PLA containing 15 wt.% I-ASE (around 80 g/10 min) explains the reason of its non spinnability.

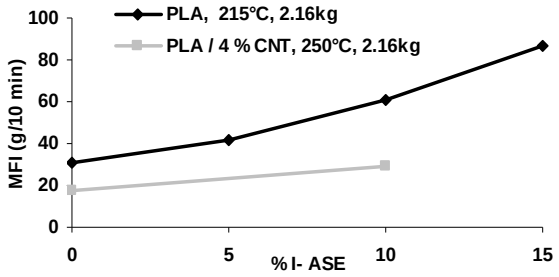

FIGURE 3. MFI of PLA and PLA/4 wt.% CNT pellets with I-ASE content.

Thermal Properties Of Pellets

PLA and PLA/4 wt.% CNTs with 5, 10 and 15 wt.% of plasticizer I-ASE were analyzed by DSC. For each blend, the second heating scan was studied and used for T_g, T_{cc}, T_m and X_c determinations. *Figures 4a* and

4b present the thermograms of PLA and PLA/CNTs blend with various amounts of plasticizer.

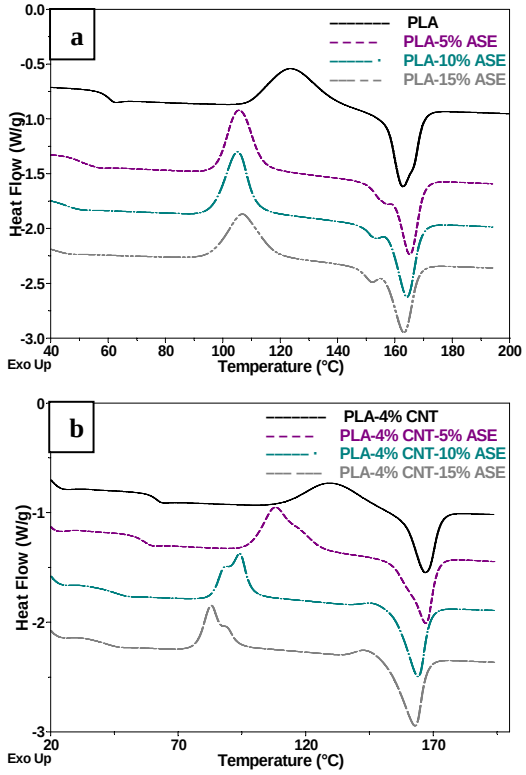

FIGURE 4. Thermograms of PLA (a) and PLA/4 wt.% CNT (b) pellets with various contents of I-ASE.

In the presence of plasticizer, two distinct peaks in the melting endotherms for PLA and cold crystallisation exotherms for PLA/CNTs appear. Nijenhuis *et al.*[40] reported this behaviour as a result of lamellar rearrangement during crystallization of PLA. A shoulder or a lower temperature peak is observed on the melting endotherm of the original crystallites. Cartier *et al*[41] described in literature the different crystalline structures of PLA.

Concerning the glass transition temperature (T_g), *Figure 5* shows the strong decrease of the T_g value from 60°C to 40°C with increasing plasticizer content. The presence of a plasticizer decreases the glass transition of PLA, improving its ductibility and drawability, thus broadening the range of potential applications[42]. The plasticizer decreases also the cold crystallization and melting temperatures. In fact, by studying more precisely the crystallinity degree *Figure 6*, we clearly see the improvement of PLA crystallinity with the I-ASE increase.

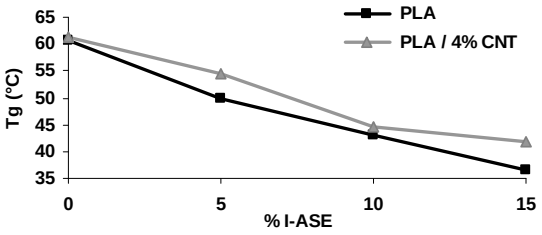

FIGURE 5. Glass transition temperature of PLA and PLA/4 wt.% CNT pellets with I-ASE.

Due to the enhancement of the chain mobility, the plasticizer increases the ability of PLA to crystallize[43]. The temperature of cold crystallisation was decreased and the crystallization peak was narrowed which was again enhanced by the higher plasticizer content. *Figure 6* shows also the higher crystallinity of PLA containing CNT than pure PLA. The nucleating agent effect of CNTs on PLA is well established[44], but the introduction of plasticizer in PLA/CNT blends enhances again the PLA crystallinity. Combining nucleating agents and plasticizers leads to a synergistic effect on PLA crystallization kinetics due the improved chain mobility and the enhanced nucleating ability[45].

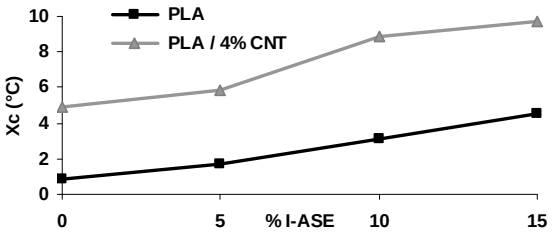

FIGURE 6. Crystallinity of PLA and PLA/4 wt.% CNT pellets with I-ASE.

Fibres: Influence Of Spinning Conditions

Table I summarizes all the spinning conditions and yarns obtained for this study. The influence of the spinning parameters on PLA crystallinity was first analyzed. In fact, compared to PLA, spinning parameters of PLA containing carbon nanotubes had to be totally changed to obtain thicker monofilaments, in order to maintain a satisfactory electrical conductivity with the smaller diameter of fibre. In this way, the temperature (T_2) and the speed (S_2) of the drawing roll have to be reduced. *Figure 7* and *8* show the cold crystallisation and the crystallinity of PLA fibres at T_2 = 90°C and 110°C depending on the drawing roll speed.

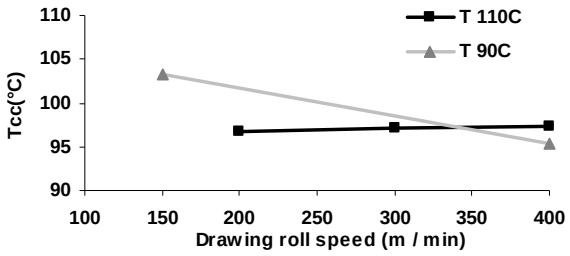

FIGURE 7. Cold crystallisation temperature of PLA fibres at T_2 = 90°C and 110°C depending on S_2.

At 90°C, cold crystallization temperature decreases from 103°C to 95°C at 150 and 400 m/min respectively, and the degree of crystallinity increases from 12 to 15% at the same roll speeds. In fact, the higher orientation of the macromolecular chains with drawing favours the PLA crystallization during the spinning process by decreasing T_{cc} and increasing X_c. At the opposite, when T_2 was fixed at 110°C, the inverse crystallinity behaviour is observed. T_{cc} slowly increases with drawing roll speed and X_c decreases from 51 to 41% at 150 and 400 m/min. In fact, a low speed and a high temperature allow a thermal treatment of PLA which favours its crystallization.

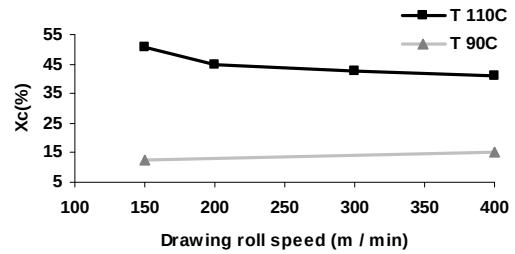

FIGURE 8. Crystallinity of fibres at T_2 = 90°C and 110°C depending on S_2.

Concerning fibres containing plasticizer, same results, as seen previously with the pellets study on the glass transition temperature and crystallinity, were highlighted. *Figure 9* and *10* show the T_g values and the degree of crystallinity of PLA and PLA/4 wt.% CNTs fibres with various amounts of I-ASE. The glass transition temperature decreases with increasing plasticizer but no influence of the spinning process conditions was observed.

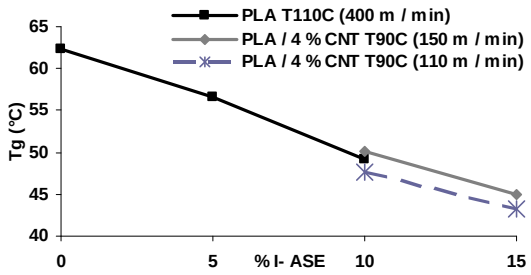

FIGURE 9. . Glass transition temperature of PLA and PLA/4 wt.% CNTs yarns containing plasticizer.

The PLA crystallinity increases with the plasticizer content. In the PLA case, the crystallinity increases in the order of 3% from 0 to 10 wt.% of I-ASE. A 3% enhancement of crystallinity is also observed for the PLA/CNTs fibres from 10 to 15 wt.% I-ASE. The higher molecular chains mobility can also explain the improvement of the crystallinity in the yarn. A crystallinity difference of 15% is observed between PLA and PLA/CNT fibres having both 10 wt.% of I-ASE. This is mainly due to higher drawing roll temperature applied during the PLA spinning process.

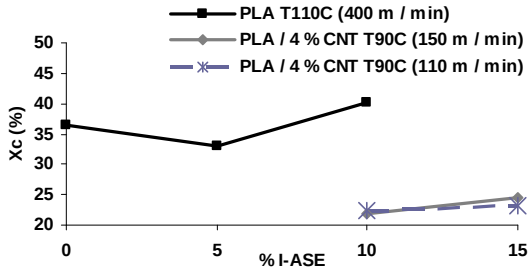

FIGURE 10. Crystallinity of PLA and PLA/4 wt.% CNTs yarns containing plasticizer.

Mechanical Properties Of Fibres

Tensile properties of PLA by varying the drawing roll parameters were first investigated. It is well known that higher crystalline is for a polymer, higher are the Young's modulus and the tensile strength and lower is the elongation at break. *Figures 11, 12* and *13* represent Young's modulus, tensile strength and elongation at break of PLA fibres respectively, as function of the drawing roll speed.

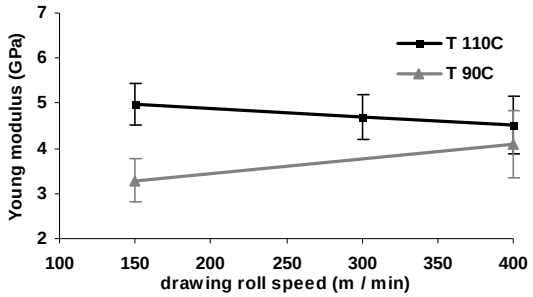

FIGURE 11. Young's modulus of PLA fibres at T_2 = 90°C and 110°C depending on S_2.

At a temperature equal to 90°C for the second drawing rate, Young's modulus of PLA increases from 3.3 to 4.1 GPa at 150 and 400 m/min respectively. Tensile strength enhances from 153 to 195 MPa and the elongation at break decreases from 142 to 53% at the same speeds. These results can be logically related to the crystallinity results. The PLA crystallinity improves the modulus and the tensile strength and decrease the elongation. At a temperature equal to 110°C for the second roll, we can notice a higher Young'modulus than for a roll temperature equal to 90°C (5 GPa versus 3.3 GPa). The long residence time of the filaments on the higher temperature roll explains the improvement of the crystallinity at low speed and so the improvement of the tensile properties. When the drawing roll speed increases, we observed the opposite behaviour than previously, corresponding to a decrease of the Young's modulus (from 5 to 4.5 GPa) and of the tensile strength (from 230 to 195 MPa) and an increase of the elongation at break (from 37 to 53%). These results can be related to the crystallinity results. The most interesting result of these mechanical analyses is the similar value at 110°C and 90°C we obtained at 400 m/min for all the mechanical data. The decrease of T_2 mainly affects the mechanical properties under 400 m/min and particularly at very low speed.

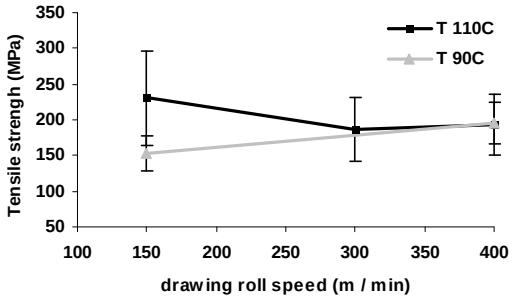

FIGURE 12. Tensile strength of PLA fibres at T_2 = 90°C and 110°C depending on S_2.

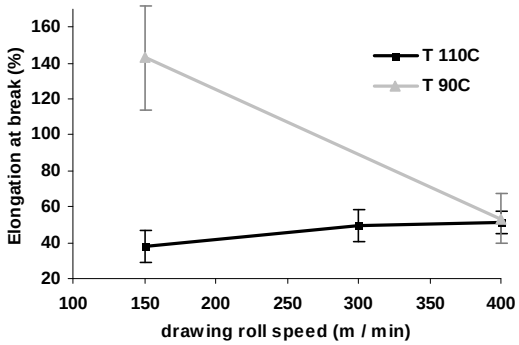

FIGURE 13. Elongation at break of PLA fibres at T_2 = 90°C and 110°C depending on S_2.

The same mechanical tests were performed for PLA and PLA/4 wt.% CNTs containing various amounts of I-ASE to understand the plasticizer influence on mechanical properties of PLA and blends. *Figures 14, 15* and *16* represent respectively Young's modulus, tensile strength and elongation at break of PLA and PLA/4 wt.% CNTs fibres depending on the I-ASE content. Plasticizer generally decreases the Young's modulus and the tensile strength and increases the elongation at break[36-37]. However in the case of slowly crystallizing polymers such as PLA, the increase of crystallinity due to enhanced chain mobility can partially or completely offset the plasticization effect[45]. This explains the enhancement of the Young's modulus and the tensile strength with the plasticizer content because of the crystallinity increase of PLA.

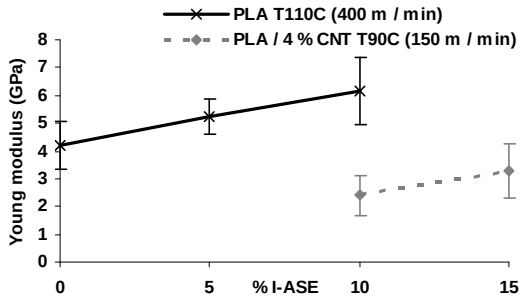

FIGURE 14. Young's modulus of PLA and PLA 4 wt.% CNTs fibres at various content of I-ASE.

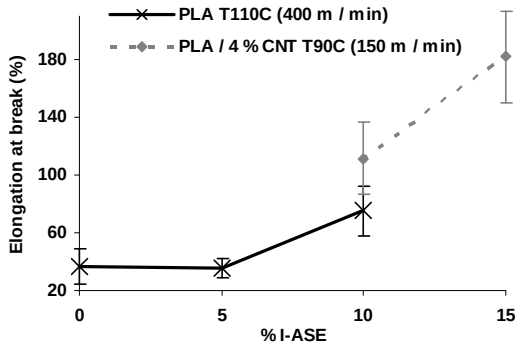

FIGURE 15. Tensile strength of PLA and PLA/4 wt.% CNTs fibres at various content of I-ASE.

Regarding the elongation at break, a strong increase is observed from a plasticizer amount of 10%. Even a high degree of crystallinity which improves the mechanical properties, the elongation at break is still increased with the plasticizer. So, a plasticizer proved to be necessary to allow spinning PLA fibres with 4 wt.% CNTs with suitable elongation.

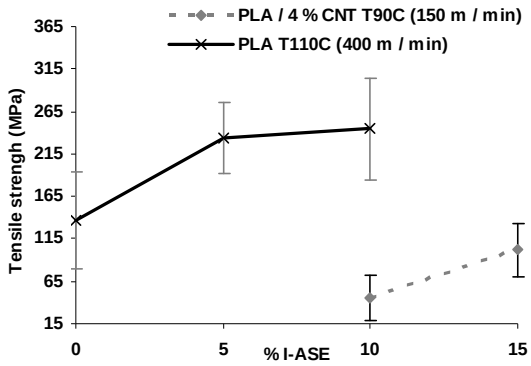

FIGURE 16. Elongation at break of PLA and PLA/4 wt.% CNTs fibres at various content of I-ASE.

Electrical And Humidity Sensing Properties Of Fibres

Four different multifilament yarns with suitable diameter were obtained. *Table II* shows the resistance value of the yarns depending on the plasticizer content and drawing roll speed.

TABLE II. Resistance of the conductive multifilament yarns.

Draw roll speed (m/min)	Resistance (kΩ / cm)	
	PLA / 4 % CNT / 10 % ASE	PLA / 4 % CNT / 15 % ASE
150	400	25
110	110	15

First, the higher the plasticizer content is, the lower is the yarn resistance. The presence of the plasticizer increases the electrical conductivity of the fibres. Secondly, the increase of the drawing roll speed enhances the fibres resistance. In fact, the drawing of the fibre decreases the electrical conductivity by increasing the intertube distance and partially breaking the conductive nanotubes network. These fibres were tested in the climatic chamber with various percentages of relative humidity to determine their humidity sensitivity *Figure 17*.

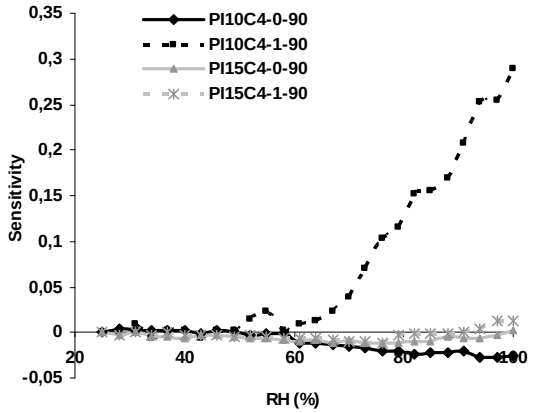

FIGURE 17. Relative humidity sensitivity of conductive multifilament yarns (see the corresponding codes of each sample in Table I).

Only the yarn having the higher resistance (PLA/4 wt.% CNTs/10 wt.% I-ASE drawn at 150 m/min) seems to be sensitive to vapour water with an increase from 70 RH% to reach a sensitivity close to 0.3 at 100 RH%. The sensitivity enhancement, corresponding to an increase of the electrical conductivity, can be attributed to the increase of conductive paths number in PLA in the presence of water. According to Yang *et al.*[46], two processes are responsible for the reduction of the resistance. The first is related to the water electrolysis, which occurs on the anode and cathode, and the second process is connected to the transport of H^+ ions, produced at the anode through the polymer towards the cathode. The presence of absorbed water in the polymer allows not only electrolysis but also reduces the ionic interaction between the polar groups of the polymer and the H^+ ions which in turns increases the ion mobility. Regarding the sensitivity of the other conductive yarns, we can see that the presence of humidity does not change the electrical response of the higher conductive fibres. Over the percolation threshold, PLA/CNTs blends are too conductive to allow a resistance change with the presence of water. Water vapour does not disturb the electrical properties of

high conductive blends. To obtain a sensitive multifilament yarn containing 4 wt.% of CNTs, it is necessary to reach the percolation field by increasing the drawing roll speed to produce thinner monofilaments. The plasticizer content and the spinning conditions of sample PI10C4-1-90 are the most adapted in producing vapour water sensitive yarn.

Four 100% relative humidity cycles were realized on this yarn to determine the repeatability and the reversibility of the electrical response. *Figure 18* shows the resulting sensitivity.

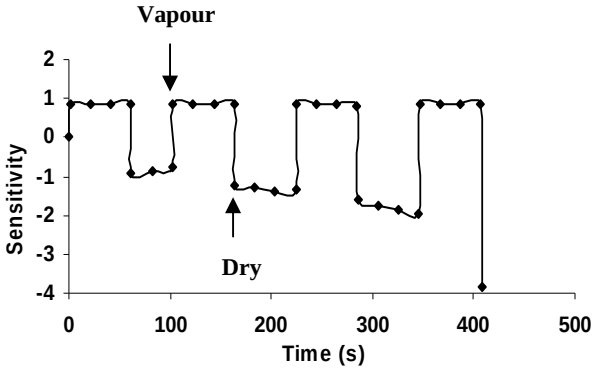

FIGURE 18. 100 RH% sensitivity of PI10C4-1-90 fibre.

The first vapour water absorption implies an enhancement of the sensitivity close to 1. When the humidity is removed, the decrease of the sensitivity is observed. This phenomenon highlights the fast reversibility of the electrical response, corresponding to a decrease of the electrical conductivity without water. After this first 100 RH% treatment, the final sensitivity of the fibre is close to -1; the resistance of the sensitive yarn at room RH (around 35 RH%) is higher after the humidity treatment. The 100 RH% treatment decreases the electrical conductivity of the multifilament at room relative humidity. After this, the three consecutive treatments realized show the same results concerning the fast signal reversibility and the resistance decrease after humidity treatment. The sensitivity to vapour water seems to be constant after few cycles and indicates that this sensitive yarn can be used more than four times for the humidity detection.

CONCLUSION

Polylactide (PLA)/carbon nanotubes (CNTs) blends were produced by extrusion process in order to elaborate new humidity sensor multifilament yarns by melt spinning process. In previous work a percolation curve in diameter of PLA monofilament containing 4 wt.% CNTs was determined and the acceptable electrical conductivity for detection was reached for a minimum diameter of 80 µm. To obtain a multifilament yarn composed by monofilaments having this diameter, the melt spinning conditions have to be adapted by reducing the drawing roll speed. In this way the temperature and the speed of the drawing roll were studied and their influence on the crystallinity and the mechanical properties of pure PLA multifilament yarns were highlighted. At low drawing roll temperature (90°C), higher the drawing roll speed is, higher are the crystallinity, the Young's modulus and the tensile strength of PLA multifilament. This is due to higher macromolecular chains orientation with drawing. At the opposite at high drawing roll temperature (110°C), higher the drawing roll speed is, lower are the crystallinity, the Young's modulus and the tensile strength of PLA fibres. This contrary phenomenon can be explained by the long resident time of the fibres on the second roll. In fact a low speed and a high temperature allow a thermal treatment of PLA which favours its crystallization.

To obtain conductive multifilament yarns, it is necessary to introduce 4 wt.% CNTs but the very high viscosity of this blend needs the use of a plasticizer to decrease the glass transition temperature and to increase the fluidity and the drawability. Various contents of plasticizer were introduced in PLA and PLA/4 wt.% CNTs blend. In both cases the presence of the plasticizer increases the PLA crystallinity and enhances the mechanical properties by increasing the Young's modulus, the tensile strength and the elongation at break of the filaments. PLA/4 wt.% CNTs multifilament yarns containing 10 and 15 wt.% of plasticizer were produced, both with 2 different drawing roll speed. The plasticizer content and the drawing speed influence the electrical conductivity of the yarns. Increasing plasticizer enhances the conductivity when increasing roll rate decreases the conductivity. The drawing of the fibres decreases the electrical conductivity by increasing the intertube distance and partially breaking the nanotubes network. These multifilaments were placed in climatic chamber to test their sensitivity to water vapour. Only the lower conductive fibre shows humidity sensitivity thanks to its lower diameter. In fact the too conductive yarns are over the percolation and the humidity does not disturb enough the electrical properties to be observed. It cannot improve the electrical conductivity of very conductive sample. The sensitive fibre, PLA/4 wt.% CNTs/10 wt.% I-ASE produced at 150 m/min, was tested along four consecutive humidity cycles. The repeatability and the fast reversibility of the sensitivity from room

relative humidity to 100 RH% were demonstrated. This multifilament yarn can be integrated in a textile fabric produce a new textile humidity sensor.

REFERENCES

[1] Tsuji, H.; Ikada, Y.; Properties and morphologies of poly (L-lactide acid): 1. Annealing condition effects on properties and morphologies of poly (L-lactide acid); *Polymer* 1995, 36, 2709-2716.

[2] Di Lorenzo, M.L.; Determination of spherulite growth rates of poly(L-lactide acid) using combined isothermal and non-isothermal procedures, *Polymer* 2001, 42, 9441-9446.

[3] Solarski, S.; Mahjoubi, F.; Ferreira, M.; Devaux, E.; Bachelet, P.; Bourbigot, S.; Delobel, R.; Coszach, P.; Murariu, M.; Da silva Ferreira, A.; Alexandre, M.; Degee, P.; Dubois, P.; Plasticized Polylactide/clay nanocomposite textile: thermal, mechanical, shrinkage and fire properties, *Journal of Materials Science* 2007, 42, 5105-5117.

[4] Wu, C.S.; Liao, H.T.; Study on the preparation and characterization of biodegradable polylactide/multi-walled carbon nanotubes nanocomposites, *Polymer* 2007, 48, 4449-4458.

[5] Paul, M.A.; Delcourt, C.; Alexandre, M. ; Degee, P.; Monteverde, F.; Dubois, P.; Polylactide/montmorillonite nanocomposites : study of the hydrolytic degradation, *Polymer Degradation and Stability* 2005, 87, 535-542.

[6] Bourbigot, S.; Fontaine, G.; Flame retardancy of polylactide: an overview, *Polymer Chemistry* 2010, 1, 1413-1422.

[7] Iijima, S.; Helical microtubules of graphitic carbon, *Nature* 1991, 354, 56-58.

[8] Zhang, Q.; Rastogi, S.; Chen, D.; Lippits, D.; Lemstra, P. J.; Low percolation threshold in single-walled carbon nanotube/high density polyethylene composites prepared by melt processing technique; *Carbon* 2006, 44, 778-785.

[9] Liang, G. D.; Tjong, S. C.; Electrical properties of low-density polyethylene/multiwalles carbon nanotube nanocomposites; *Materials Chemistry and Physics* 2006, 100, 132-137.

[10] Bai, J. B.; Allaoui, A.; Effect of the length and the aggregate size of MWNTs on the improvement efficiency of the mechanical and electrical properties of nanocomposites-experimental investigation *Composites: Part A* 2003, 34, 689-694.

[11] Yang, J. ; Lin, Y. ; Wang, J.; Lai, M.; Li, J. ; Liu, J. ; Tong, X. ; Cheng, H.; Morphology, thermal stability, and dynamic mechanical properties of atactic polypropylene/carbon nanotube composites; *Journal of Applied polymer Science* 2005, 98, 1087-1091.

[12] Kashiwagi, T.; Grulke, E.; Hilding, J.; Harris, R.; Awad, W.; Douglas J.; Thermal degradation and flammability properties of poly (propylene)/carbon nanotube composites; *Macromolecular Rapid Communications* 2002, 23, 761-765.

[13] Schartel, B.; Pötschke, P.; Knoll, U.; Abdel-Goad, M.; Fire behaviour of polyamide 6/multiwall carbon nanotubes nanocomposites; *European Polymer Journal* 2005, 41, 1061-1070.

[14] Dujardin, E.; Ebbesen, T.W.; Hiura, H.; Tanigaki, K.; Capillarity and wetting of carbon nanotubes, *Science* 1994, 265, 1850-1852.

[15] Dillon, A.C.; Jones, K.M.; Bekkedahl, T.A.; Kiang, C.H.; Bethune, D.S.; Heben, M.: Storage of hydrogen in single-walled carbon nanotubes, *Nature* 1997, 386, 377-379.

[16] Kong, J.; Franhlin, N.R.; Zhou, C.; Chapline, M.G.; Peng, S.; Cho, K.; Dai, H.; Nanotube molecular wires as chemical sensors, *Science* 2000, 287, 622-625.

[17] Li, Y.; Wang, H.; Chen, Y.; Yang, M.; A multi-walled carbon nanotube/palladium nanocomposite prepared by a facile method for the detection of methane at room temperature, *Sensors and actuators B: Chemical* 2008, 132, 155-158.

[18] Valentini, L.; Cantalini, C.; Armentano, I.; Kenny, J.M.; Lozzi, L.; Santucci, S.; Highly sensitive and selective sensors based on carbon nanotubes thin films for molecular detection, *Diamond Related Materials* 2004, 13, 1301-1305.

[19] Ong, K.G.; Zeng, K.; Grimes, C.A.; A wireless, passive carbon nanotube-based gas sensor, IEEE Sensors Journal 2002,. 2, 82-88.

[20] Chopra, S.; Pham, A.; Gaillard, J.; Parker, A.; Rao, A.M.; Carbon-nanotube-based resonant-circuit sensor for ammonia, Applied Physics Letters 2002, 80, 4632-4634.

[21] Lee, J.H., Kim, J.; Seo, H.W.; Song, J.W.; Lee, E.S.; Won, M.; Han, C.S.; Bias modulated highly sensitive NO_2 gas detection using carbon nanotubes, *Sensors and Actuators B : Chemical 2008*, 129, 628-631.

[22] Varghese, O.K.; Kichambre, P.D.; Gong, D.; Ong, K.G.; Dickey, E.C.; Grimes, C.A.; Gas sensing characteristics of multi-wall carbon nanotubes, *Sensors and Actuators B : Chemical* 2001, 81, 32-41.

[23] Valentini, L.; Bavastrello, V.; Stura, E.; Armentano, I.; Nicolini, C.; Kenny, J.M.; Sensors for inorganic vapor detection based on carbon nanotubes and poly(o-anisidine) nanocomposite material, *Chemical Physics Letters* 2004, 383, 617-622.

[24] Niu, L.; Luo, Y.; Li, Z.; A highly selective chemical gas sensor based on functionnalization of multi-walled carbon nanotubes with poly(ethylene glycol), *Sensors and Actuators B : Chemical* 2007, 126, 361-367.

[25] Su, P.G.; Wang, C.S.; In situ synthesized composite thin films of MWCNTs/PMMA doped with KOH as a resistive humidity sensor, *Sensors and Actuators B: Chemical* 2007, 24, 303-308.

[26] Abraham, J.K.; Philip, B.; Witchurch, A.; Varadan, V.K.; Reddy, C.C.; A compact wireless gas sensor using a carbon nanotube/PMMA thin film chemresistor, *Smart Materials and Structures* 2004, 13,1045-1049.

[27] Zhang, B.; Fu, R.W.; Zhang, M.Q.; Dong, X.M.; Lan, P.L.; Qiu, J.S.; Preparation and characterization of gas-sensitive composites from multi-walled carbon nanotubes/polystyrene, *Sensors and Actuators B: Chemical* 2005, 109, 323-328.

[28] Wang, H.C.; Li, Y.; Yang, M.J.; Sensors for organic vapour detection based on composites of carbon nanotubes functionalized with polymers, *Sensors and Actuators B: Chemical* 2007, 124, 360-367.

[29] Kobashi, K.; Villmow, T.; Andres, T.; Pötschke, P.; Liquid sensing of melt-processed poly(lactid acic)/multi-walled carbon nanotube composite films, Sensors and Actuators B: Chemical 2008, 134, 787-795.

[30] Takasaki, M.; Ito, H.; Kikutani, T.; Structure development of polylactides with various d-lactide contents in the High-Speed Melt Spinning Process, *Journal of Macromolecular Science, Part B: Physics* 2003, 42, 57-73.

[31] Fambri, L.; Pegoretti, A.; Fenner, R.; Incardona, S.D.; Migliaseri, C; Biodegradable fibres of poly(L-lactic acid) produced by melt spinning, *Polymer* 1997, 38, 79-85.

[32] Cicero, J.A.; Dorgan, J.R.; Decc, S.F.; Knauss, D.M.; Phosphite stabilization effects on two-step melt-spun fibres of polylactide, *Polymer Degradation and Stability* 2002, 78, 95-105.

[33] Solarski, S.; Ferreira, M.; Devaux, E.; Characterization of the thermal properties of PLA fibres bymodulated differential scanning calorimetry, *Polymer* 2005, 46, 11187-11192.

[34] Pluta, M.; Morphology and properties of polylactide modified by thermal treatment, filling with layered silicates and plasticization, *Polymer* 2004, 45, 8239-8251.

[35] Paul, M.A.; Alexande, M.; Degée, P.; Monteverde, F.; Rulmont, A.; Dubois, P.; (Plasticized) polylactide/(organo-)clay nanocomposites by in situ intercalative polymerization, Macromolecular *Chemistry and Physics* 2005, 206, 484-498.

[36] Martin, O.; Avérous, L.; Poly (lactic acid): plasticization and properties of biodegradable multiphase systems, *Polymer* 2001, 42, 6209-6219.

[37] Baiardo, M.; Frisoni, G.; Scandola, M.; Rimelen, M.; Lis, D.; Ruffieux, K.; Wintermantel, E.; Thermal and mechanical properties of plasticized poly(L-lactic acid), *Journal of applied polymer Science* 2003, 90, 1731-1738.

[38] Ljungberg, N.; Wesslen, B.; The effects of plasticizers on the dynamic mechanical and thermal properties of poly (lactic acid), *Journal of applied polymer Science* 2002, 86, 1227-1234.

[39] Aubry, C.; Développement et mise en oeuvre de structures textiles contenant des nanotubes de carbone. Application aux capteurs chimiques pour la detection de solvants, *PhD dissertation* 2009, University of Lille, France.

[40] Nijenhuis, A.J.; Colstee, E.; Grijpma, D.W.; Pennings, A.J.; High molecular weight poly (l -lactide) and poly (ethylene oxide) blends: thermal characterization and physical properties, *Polymer* 1996, 37, 5849-5857.

[41] Cartier L.; Okihara T.; Ikada, Y.;, Tsuji, H.; Puiggali, J.; Lotz, B.; Epitaxial crystallization and crystalline polymorphism of polylactides, *Polymer* 2000, 41, 8909-8919.

[42] Kulinski Z.; Piorkowska, E.; Crystallization, structure and properties of plasticized poly (l-lactide), *Polymer* 2005, 46, 10290-10300.
[43] Hu, Y.; Hu, Y.S.; Topolkaraev, V.; Hiltner, A.; Baer E.; Crystallization and phase separation in blends of high stereoregular poly(lactide) with poly(ethylene glycol), *Polymer* 2003, 44, 5681-5689.
[44] Tsuji, H.; Kawashima, Y.; Takikawa, H.; Tanaka S.; Poly (l-lactide)/nano-structured carbon composites: Conductivity, thermal properties, crystallization, and biodegradation, *Polymer* 2007, 48, 4213-4225.
[45] Li, H.; Hainault, M.A.; Effect of nucleation and plasticization on the crystallization of poly(lactic acid), *Polymer* 2007, 48, 6855-6866.
[46] Yang, M.J.; Sun, H.M.; G. Casalbore-Miceli, G.; Camaioni, N.; Mari, C.M.; Poly(propargyl alcohol) doped with sulphuric acid, a new proton conductor usable for humidity sensor construction, Synthetic Metals 1996, 81, 65-69.

AUTOHORS' ADDRESSES

Eric Devaux
Carole Aubry
Christine Campagne
Maryline Rochery
FRANCE ENSAIT, GEMTEX Laboratory
2 allee Louise et Victor Champier
Roubaix, none 59056
FRANCE